Single-diffractive production of dijets within the k_t-factorization approach

Marta Łuszczak,[1,*] Rafał Maciuła,[2,†] Antoni Szczurek,[2,‡] and Izabela Babiarz[1,§]

[1]*Faculty of Mathematics and Natural Sciences, University of Rzeszów, PL-35-959 Rzeszów, Poland*

[2]*Institute of Nuclear Physics PAN, PL-31-342 Cracow, Poland*

(Received 14 July 2017; published 20 September 2017)

We discuss single-diffractive production of dijets. The cross section is calculated within the resolved Pomeron picture, for the first time in the k_t-factorization approach, neglecting transverse momentum of the Pomeron. We use Kimber-Martin-Ryskin unintegrated parton (gluon, quark, antiquark) distributions in both the proton as well as in the Pomeron or subleading Reggeon. The unintegrated parton distributions are calculated based on conventional MMHT2014nlo parton distribution functions in the proton and H1 Collaboration diffractive parton distribution functions used previously in the analysis of diffractive structure function and dijets at HERA. For comparison, we present results of calculations performed within the collinear-factorization approach. Our results remain those obtained in the next-to-leading-order approach. The calculation is (must be) supplemented by the so-called gap survival factor, which may, in general, depend on kinematical variables. We try to describe the existing data from Tevatron and make detailed predictions for possible LHC measurements. Several differential distributions are calculated. The $\bar{E}_T$, $\bar{\eta}$ and $x_{\bar{p}}$ distributions are compared with the Tevatron data. A reasonable agreement is obtained for the first two distributions. The last one requires introducing a gap survival factor which depends on kinematical variables. We discuss how the phenomenological dependence on one kinematical variable may influence dependence on other variables such as $\bar{E}_T$ and $\bar{\eta}$. Several distributions for the LHC are shown.

DOI: 10.1103/PhysRevD.96.054018

I. INTRODUCTION

The hard diffractive processes are related to the production of a system with large mass (gauge boson, Higgs boson), or large invariant mass (dijets), and the presence of a rapidity gap somewhere in rapidity space. Several hard diffractive processes have been studied in the past. The gap may be in different places with respect to final-state objects, e.g., between a forwardly produced proton and a hard system (hard single-diffractive process) or between jets (jet-gap-jet topology) or quarkonia (quarkonium-gap-quarkonium). Another category is exclusive diffractive processes (Higgs, dijets, $\gamma\gamma$, pair of heavy quarks $Q\bar{Q}$, etc.) Several other processes are possible in general, many of them not studied so far.

In the present paper, we discuss single-diffractive production of dijets. This process was discussed in the past for photo- and electroproduction [1–4] as well as for proton-proton or proton-antiproton collisions [5–9]. The hard single-diffractive processes are treated usually in the resolved Pomeron picture with a Pomeron being a virtual but composed (of partons) object. This picture was used with success for the description of hard diffractive processes studied extensively at HERA. This picture was also attempted at hadronic collisions. A few processes were studied experimentally at the Tevatron [10–20] including the dijet production.

The related calculation was performed so far in the context of the collinear-factorization approach. The corresponding parton distributions in the Pomeron, or equivalently the so-called diffractive parton distributions in the proton, have been fitted so far to the HERA data. The distributions should be universal and so, in principle, can be used in proton-proton collisions. In pp or $p\bar{p}$ collisions, the strong nonperturbative interactions can easily destroy the rapidity gap associated with Pomeron (or other color-singlet) exchange. This effect is of a nonperturbative nature and is therefore difficult to control. There were several attempts to understand the related suppression of the hard diffractive cross sections. Usually, the effect is quantified by a phenomenological gap survival factor. The factor is known to be energy dependent because the nonperturbative soft interactions are known to be energy dependent. In general, the survival probability may depend on other kinematical variables. Recently, the gap survival factor was studied for jet-gap-jet processes [21], and the dependence on the gap sizes was discussed

*luszczak@univ.rzeszow.pl
†rafal.maciula@ifj.edu.pl
‡antoni.szczurek@ifj.edu.pl
Also at University of Rzeszów, PL-35-959 Rzeszów, Poland.
§i.babiarz@gmail.com

in the picture of multiple parton scattering. In our opinion, we are still far from the full understanding of the dynamical effect.

The k_t-factorization, originally proposed by Catani *et al.* in Refs. [22,23], was used recently for different processes at the LHC. In the present paper, we intend to treat the single-diffractive dijet production for the first time also within the k_t-factorization approach. A similar approach was used recently for the single-diffractive production of $c\bar{c}$ pairs [24]. The k_t-factorization approach was also used recently for nondiffractive dijet [25], three- [26] or even four-jet production [27,28]. In particular, we wish to compare results obtained within collinear-factorization and k_t-factorization approaches. A comparison with the Tevatron data is planned. We wish to also make predictions for the LHC.

II. SKETCH OF THE APPROACH

In this paper, we follow the theoretical framework proposed very recently by three of us in Ref. [24]. There, some new ideas for the calculation of diffractive cross sections were put forward and applied in the case of single-diffractive production of charm at the LHC. According to this approach, the standard resolved Pomeron model [29], usually based on the leading-order (LO) collinear approximation, is extended by adopting a framework of the k_t-factorization as an effective way to include higher-order corrections. It was shown several times that the k_t-factorization approach is very useful in this context and especially efficient in the studies of kinematical correlations (see, e.g., Refs. [25,30]).

A sketch of the mechanisms under consideration, relevant for the inclusive single-diffractive production of dijets in pp or $p\bar{p}$ collisions, with the notation of kinematical variables and with some theoretical ingredients used in the following is shown in Fig. 1.

According to the approach introduced above, the cross section for inclusive single-diffractive production of the dijet, for both considered diagrams (left and right panels of Fig. 1), can be written as

$$d\sigma^{SD(1)}(p_a p_b \to p_a \mathrm{dijet} XY) = \sum_{i,j,k,l} \int dx_1 \frac{d^2k_{1t}}{\pi} dx_2 \frac{d^2k_{2t}}{\pi} d\hat{\sigma}(i^* j^* \to kl) \times \mathcal{F}_i^D(x_1, k_{1t}^2, \mu^2) \cdot \mathcal{F}_j(x_2, k_{2t}^2, \mu^2), \tag{2.1}$$

$$d\sigma^{SD(2)}(p_a p_b \to \mathrm{dijet} p_b XY) = \sum_{i,j,k,l} \int dx_1 \frac{d^2k_{1t}}{\pi} dx_2 \frac{d^2k_{2t}}{\pi} d\hat{\sigma}(i^* j^* \to kl) \times \mathcal{F}_i(x_1, k_{1t}^2, \mu^2) \cdot \mathcal{F}_j^D(x_2, k_{2t}^2, \mu^2), \tag{2.2}$$

where $\mathcal{F}_i(x, k_t^2, \mu^2)$ are the "conventional" unintegrated (k_t-dependent) parton distributions (UPDFs) in the proton and $\mathcal{F}_i^D(x, k_t^2, \mu^2)$ are their diffractive counterparts—which we will call here diffractive UPDFs. The latter can be interpreted as the probability of finding a parton i with longitudinal momentum fraction x and transverse momentum (virtuality) k_t at the factorization scale μ^2 assuming that the proton which losts a momentum fraction x_{IP} remains intact.

The $2 \to 2$ partonic cross sections in Eqs. (2.1) and (2.2) read

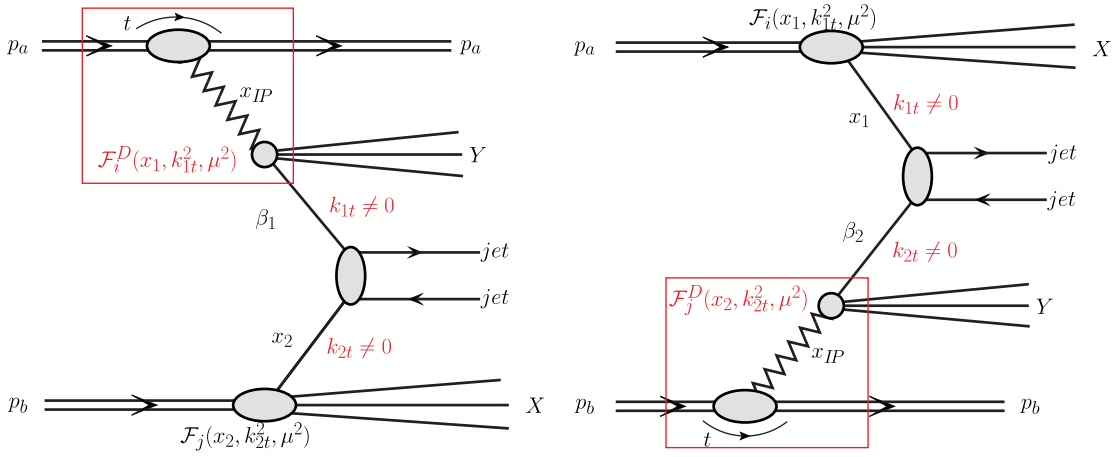

FIG. 1. A diagrammatic representation of the considered mechanisms of single-diffractive dijet production within the resolved Pomeron model extended in the present paper to the k_t-factorization approach.

$$d\hat{\sigma}(i^*j^* \to kl) = \frac{d^3p_1}{2E_1(2\pi)^3}\frac{d^3p_2}{2E_2(2\pi)^3} \times (2\pi)^2\delta^2(p_1+p_2-k_1-k_2) \times \overline{|\mathcal{M}_{i^*j^*\to kl}(k_1,k_2)|^2} \quad (2.3)$$

with $i,j,k,l = g,u,d,s,\bar{u},\bar{d},\bar{s}$, where p_1, E_1 and p_2, E_2 are the momenta and energies of outgoing partons, respectively, and $\mathcal{M}_{i^*j^*\to kl}(k_1,k_2)$ are the off-shell matrix elements for the $i^*j^* \to kl$ subprocesses with initial-state partons i and j being off mass shell. In the numerical calculations here, we include all $2 \to 2$ partonic channels:

$$\#1 = g^*g^* \to gg, \quad \#4 = g^*g^* \to q\bar{q}, \quad \#7 = q^*\bar{q}^* \to gg,$$
$$\#2 = q^*g^* \to qg, \quad \#5 = q^*\bar{q}^* \to q\bar{q}, \quad \#8 = q^*q^* \to qq,$$
$$\#3 = g^*q^* \to gq, \quad \#6 = q^*\bar{q}^* \to q'\bar{q}', \quad \#9 = q^*q'^* \to qq'.$$

The relevant gauge-invariant off-shell matrix elements for each of the channels above can be calculated, e.g., within the method of parton Reggeization. It was done recently in Ref. [25], where the matrix elements were presented in a very useful analytical form.

As we proposed very recently in Ref. [24], the diffractive UPDFs can be calculated from their collinear counterparts via the Kimber-Martin-Ryskin (KMR) method [31,32].[1] Then, the diffractive unintegrated parton distributions for the gluon and quark are given by the following formulas,

$$f_g^D(x,k_t^2,\mu^2) \equiv \frac{\partial}{\partial \log k_t^2}[g^D(x,k_t^2)T_g(k_t^2,\mu^2)] = T_g(k_t^2,\mu^2)\frac{\alpha_S(k_t^2)}{2\pi} \times \int_x^1 dz\left[\sum_q P_{gq}(z)\frac{x}{z}q^D\left(\frac{x}{z},k_t^2\right) + P_{gg}(z)\frac{x}{z}g^D\left(\frac{x}{z},k_t^2\right)\Theta(\Delta-z)\right], \quad (2.4)$$

$$f_q^D(x,k_t^2,\mu^2) \equiv \frac{\partial}{\partial \log k_t^2}[q^D(x,k_t^2)T_q(k_t^2,\mu^2)] = T_q(k_t^2,\mu^2)\frac{\alpha_S(k_t^2)}{2\pi} \times \int_x^1 dz\left[P_{qq}(z)\frac{x}{z}q^D\left(\frac{x}{z},k_t^2\right) \times \Theta(\Delta-z) + P_{qg}(z)\frac{x}{z}g^D\left(\frac{x}{z},k_t^2\right)\right], \quad (2.5)$$

[1]The KMR method is based on an earlier observation originally made by Catani *et al.* [33], where a relationship between high-energy factorization and the factorization theorem on mass singularities was established.

where g^D and q^D are the collinear diffractive parton distribution functions (PDFs) in the proton. The P_{qq}, P_{qg}, P_{gq} and P_{gg} are the usual unregulated LO Dokshitzer-Gribov-Lipatov-Altarelli-Parisi (DGLAP) splitting functions, and T_g and T_q are the gluon and quark Sudakov form factors, respectively. More details of the whole procedure and a discussion of all of the ingredients can be found, e.g., in Ref. [32].

According to the so-called proton-vertex-factorization, the diffractive collinear PDF in the proton, e.g., for the gluon, has the following generic form,

$$g^D(x,\mu^2) = \int dx_{IP}d\beta\delta(x-x_{IP}\beta)g_{IP}(\beta,\mu^2)f_{IP}(x_{IP}) = \int_x^{x^{\max}}\frac{dx_{IP}}{x_{IP}}f_{IP}(x_{IP})g_{IP}\left(\frac{x}{x_{IP}},\mu^2\right), \quad (2.6)$$

where $\beta = \frac{x}{x_{IP}}$ is the longitudinal momentum fraction of the Pomeron carried by gluon and the flux of Pomerons may be taken as

$$f_{IP}(x_{IP}) = \int_{t_{\min}}^{t_{\max}} dt f(x_{IP},t). \quad (2.7)$$

An analogous expression can also be written for the collinear diffractive quark distribution.

In this paper, the diffractive KMR UPDFs are calculated from the "H1 2006 fit A" diffractive collinear PDFs [34], that are only available at next-to-leading order. In the calculation of the conventional nondiffractive KMR UPDFs, the collinear MMHT2014nlo PDFs [35] were used. In the perturbative part of the calculations, we take running coupling constant $\alpha_S(\mu_R^2)$ and the renormalization and factorization scales equal to $\mu^2 = \mu_R^2 = \mu_F^2 = \frac{p_{1t}^2+p_{2t}^2}{2}$, where p_{1t} and p_{2t} are the transverse momenta of the outgoing jets.

Before starting the presentation of our results, we wish to make a comment on some limitations of k_t-factorization for jet production. In the k_T-factorization approach, the production of jets can also occur from the unintegrated PDFs. We followed this fact in our papers, when considering, e.g., $c\bar{c}$, $b\bar{b}$ or $c\bar{c}$ + jet production. These additional hard emissions lead to an effective inclusion of a part of higher-order (real) corrections (see our discussion, e.g., in Ref. [36]).

However, in the case of dijet production, the situation is a bit more complicated. The condition $k_T < p_T^{sub}$ arises from the methods of dijet experimental data analyses at the Tevatron and/or LHC. Usually, the two (p_T)-hardest jets (the two most energetic) from the $n_{jet} > 2$ sample are taken into account. Experimentally, it is impossible to separate final-state partons/jets produced in the hard-parton scattering from the ones generated during the evolution of uPDFs. In the KMR method, the situations where $k_T > p_T^{sub}$ or even $k_T > p_T^{lead}$ are possible. However, the kinematics of the hard parton from the uPDF is not under full control,

and one cannot say whether it fulfills, e.g., a rapidity detector acceptance. Therefore, to avoid overestimation of the visible cross section, one needs to keep the two hardest jets coming from the hard-matrix element only. The additional emission from the uPDF is constrained but still important. The condition $k_T < p_T^{sub}$ was originally proposed in Ref. [25].

The rapidity gap is treated here in the same way for collinear and k_t-factorization as it is related to another additional (treated as independent) soft scattering. In some calculations performed here, it is just included by a multiplication of the resolved Pomeron model result by a gap survival factor. Also, when discussing the possible dependence of the gap survival on $x_{\bar{p}}$ (see Sec. III .B), we use a similar fitting function adjusted to the Tevatron experimental data. In this case, however, the parameters of the fitting function are different, which means that the gap survival factor is different for the collinear and k_t-factorization approach.

III. RESULTS

In this section, we shall show results of our calculations. We shall start from a trial of the description of the Tevatron experimental data [13,14].

A. Tevatron cuts

We start by showing our results for $\bar{E}_T = \frac{E_{1T}+E_{2T}}{2}$ and $\bar{\eta} = \frac{\eta_1+\eta_2}{2}$ distributions; see Fig. 2. In this calculation, the Pomeron/Reggeon longitudinal momentum fraction was limited as in the experimental case [13,14] to $0.035 < x_{IP,IR} < 0.095$. We show both the naive result obtained with the KMR UGDF (dashed line) as well as similar results with limitations on parton transverse momenta $k_T < p_T^{sub}$ (solid line) and $k_T < 7$ TeV (dash-dotted line). Above, p_T^{sub} is the transverse momentum of the subleading jet. The first limitation was proposed for standard non-diffractive jets [25]. The latter limitation is related to the lower experimental cut on jet transverse momenta. For comparison, we show also the distribution obtained in the leading-order collinear-factorization approach (dotted line). A large difference can be seen close to the lower transverse momentum cut. A similar effect was discussed recently for four-jet production in Ref. [27].

Figure 3 shows somewhat theoretical two-dimensional distribution in transverse momenta of partons. Surprisingly, the distribution is almost symmetric in k_{1T} and k_{2T}. The limitation on parton transverse momenta $k_T < p_T^{sub}$ makes the two-dimensional distribution much narrower, although the consequences on the distribution in transverse momenta and rapidity are not dramatic as has already been shown in Fig. 2.

In contrast to the leading-order collinear-factorization approach, in the k_t-factorization approach, the transverse momentum distributions of leading (solid) and subleading (dashed) jets differ as is shown in the left panel of Fig. 4. In contrast to the leading-order collinear-factorization approach, in the k_t-factorization approach, the transverse momentum distributions of leading (solid) and subleading (dashed) jets differ as is shown in the left panel of Fig. 4. Here, a standard cut on parton transverse momentum $k_T < p_T^{sub}$ has been imposed. In the right panel of Fig. 4, we show how the single-diffractive cross section depends on the cut on the square of four-momentum transfer to the outgoing antiproton (the antiproton was measured in the CDF experiment). The cut $|t| < 0.2$ GeV^2 changes the cross section normalization but does not modify the shape of the distribution.

Here, a standard cut on the parton transverse momentum has been imposed. The single-diffractive cross section depends on the cut on four-momentum squared transferred to the outgoing antiproton (the antiproton was measured in the CDF experiment). The cut changes the cross section normalization but does not modify the shape of the distribution.

In our calculation, we include both Pomeron and subleading Reggeon exchanges. In the selected range of x_{IP}, the Pomeron contribution is much bigger than the

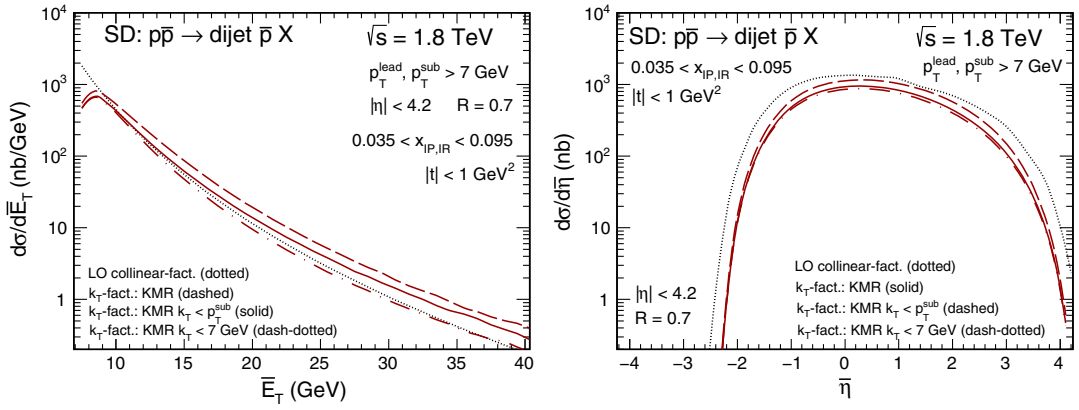

FIG. 2. Distribution in average $\bar{E}_T$ (left panel) and in average $\bar{\eta}$ (right panel). Here, $S_G = 0.1$.

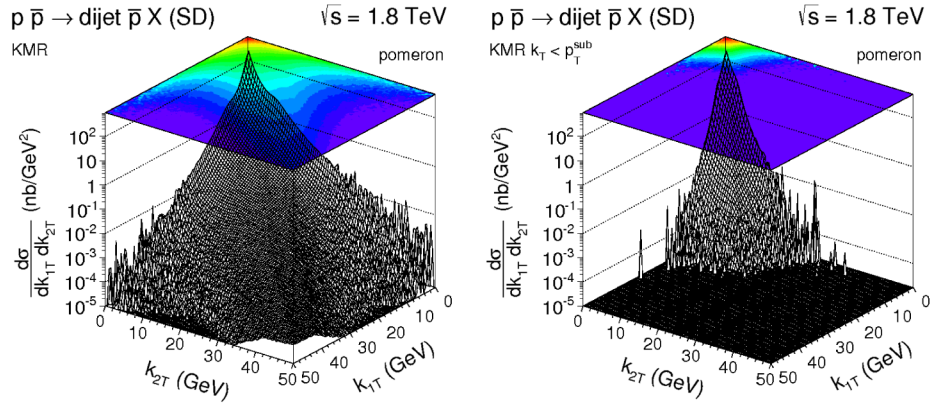

FIG. 3. Two-dimensional distribution in transverse momenta of partons on the nondiffractive side (k_{1T}) and on the diffractive side (k_{2T}). Here, $S_G = 0.1$.

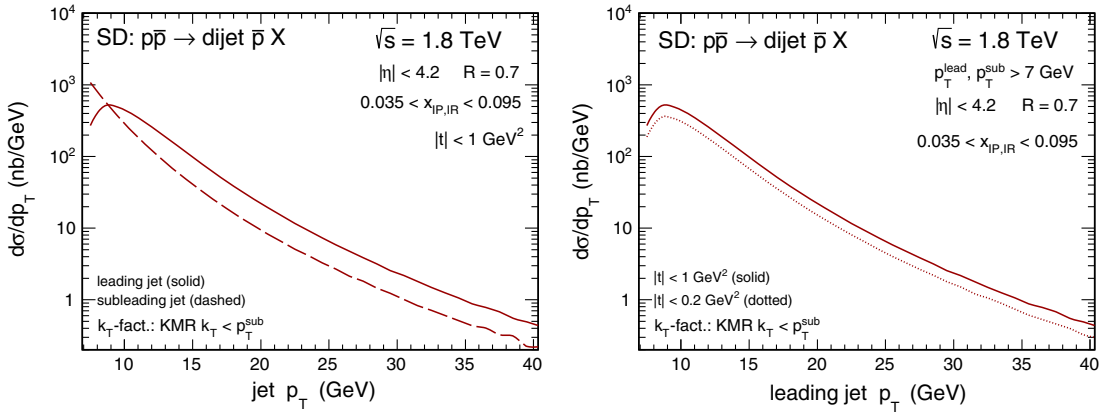

FIG. 4. Transverse momentum distribution for leading and subleading jets (left panel) and the influence of the cut on t on the leading jet (right panel). Here, $S_G = 0.1$.

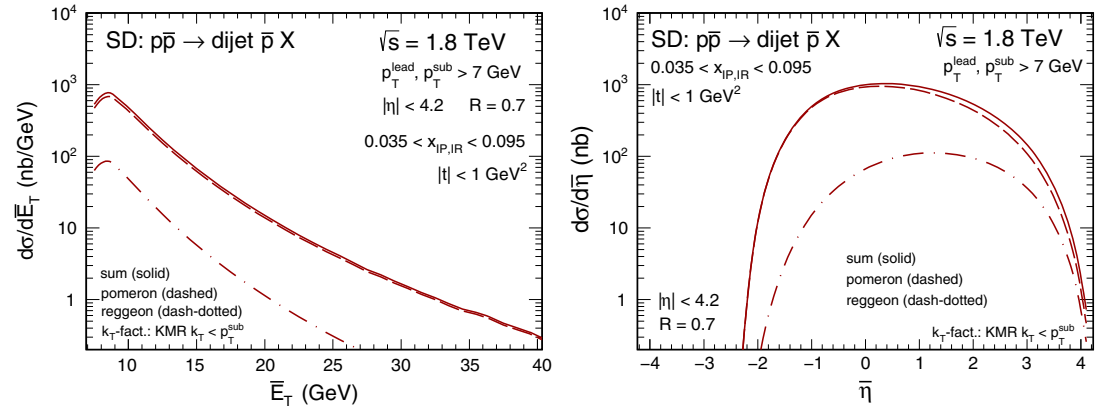

FIG. 5. The Pomeron and subleading Reggeon contribution for $\bar{E}_T$ (left panel) and $\bar{\eta}$ (right panel).

contribution of the subleading Reggeon as shown in Fig. 5. The subleading Reggeon contribution is about 10% of the single-diffractive cross section. For the average jet rapidity distribution, the situation is a bit more complicated. Both contributions are of the same order for large $\bar{\eta}$.

Now, we wish to consider distributions that can be compared to the experimental ones.

In Fig. 6, we show the distribution in $\bar{E}_T$ for two collision energies. While the k_t-factorization approach gives a better description of the data close to the lower experimental cut on jet transverse momenta, the collinear-factorization

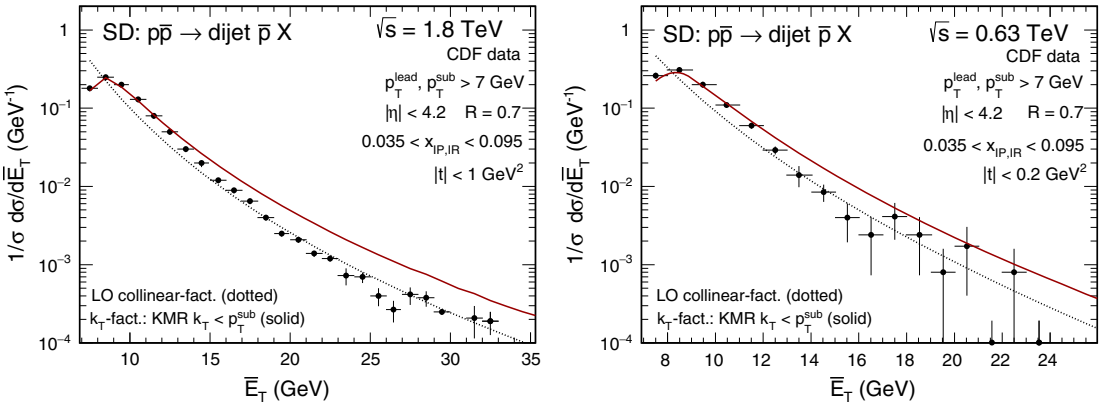

FIG. 6. The average transverse energy distribution for $\sqrt{s} = 1.8$ TeV (left panel) and for $\sqrt{s} = 630$ GeV (right panel).

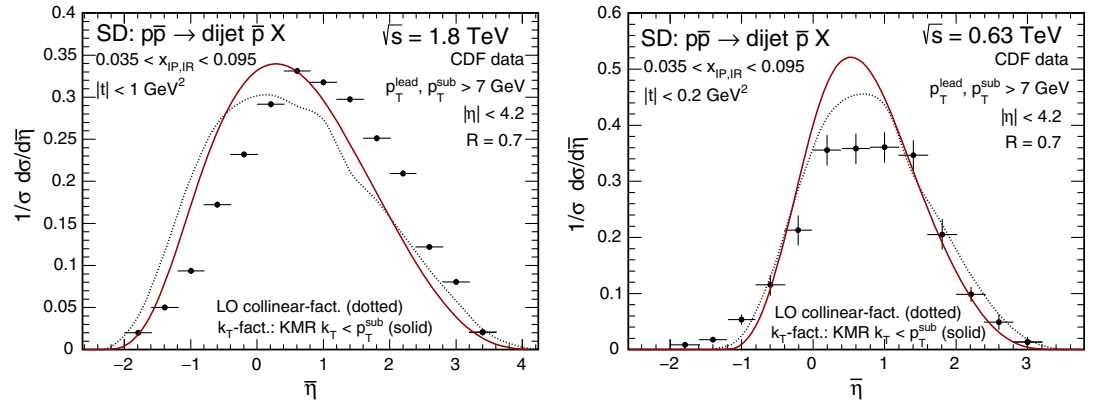

FIG. 7. The average rapidity distribution for $\sqrt{s} = 1.8$ TeV (left panel) and for $\sqrt{s} = 630$ GeV (right panel).

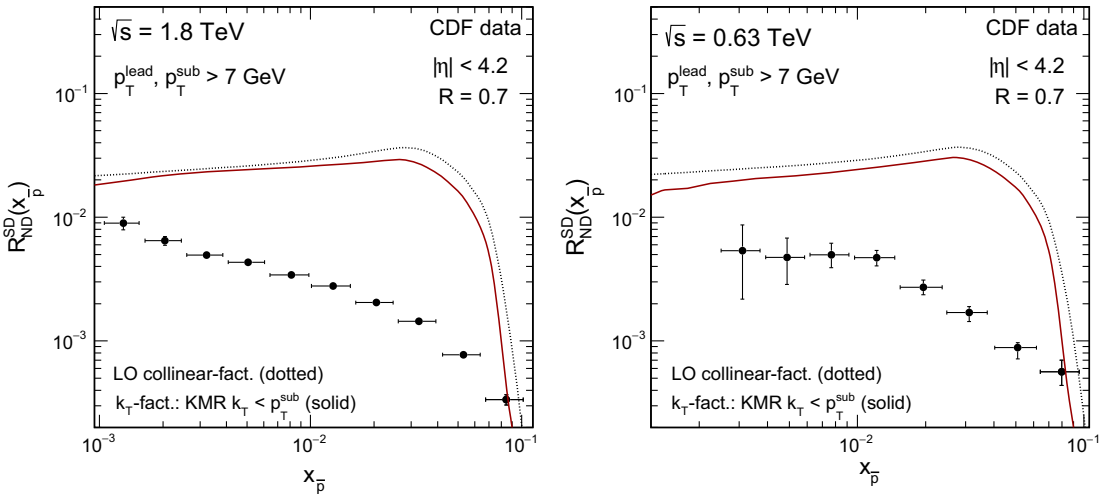

FIG. 8. Distribution in $x_{\bar{p}}$ for $\sqrt{s} = 1.8$ TeV (left panel) and for $\sqrt{s} = 630$ GeV (right panel). No gap survival factor was included here.

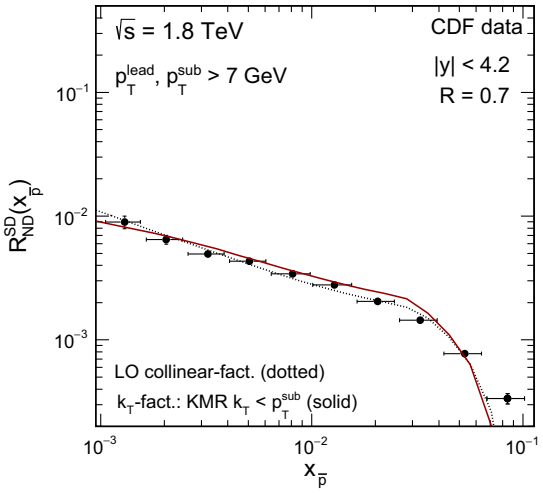

FIG. 9. The ratio of single-diffractive to nondiffractive cross sections as a function of $x_{\bar{p}}$. The lines are fits of S_G to the CDF data.

approach seems to be better for larger transverse momenta. This is true for both Tevatron collision energies. We do not have a good understanding of the result.

In Fig. 7, we show distributions in average jet rapidity again for the two collision energies. Here, the k_t-factorization result better describes the experimental data than the result obtained in the collinear approach. The outgoing antiproton is at $\eta \approx -6.05$ for $\sqrt{s} = 1.8$ TeV and $\eta \approx -5.53$ for $\sqrt{s} = 630$ GeV.

We wish to note here that both the experimental distributions in $\bar{E}_T$ and in $\bar{\eta}$ are not absolutely normalized (inspect the description y axes of Figs. 6 and 7). On the theoretical side, the absolute cross section depends on the gap survival factor, which is not easy to calculate from the first principle. The CDF Collaboration showed also the distribution in $x_{\bar{p}}$ normalized to the inclusive cross section. Our theoretical result is clearly above the experimental result; see Fig. 8. Roughly a factor of order 0.1 is missing in our calculation, although the exact shape is not exactly the same.

There can be several reasons for the disagreement of our results with the CDF data. One of them is not a perfect extraction of the diffractive distributions at HERA. Another one is the dependence of the gap survival factor on kinematical variables. This possibility will be discussed now in the next subsection.

B. Kinematical dependence of gap survival factor

In this section, we assume that the gap survival factor is a function of $x_{\bar{p}}$ only. This assumption is a bit academic, but we wish to see a possible influence of such a dependence on other distributions. In Fig. 9, we show a fit to the data assuming some functional form for $S_G(x_{\bar{p}})$, $S_G(x_{\bar{p}}) = 0.0056 * (x_{\bar{p}}^{-0.6} + x_{\bar{p}}^{-0.02})$ for the collinear case and $S_G(x_{\bar{p}}) = 0.004 * (x_{\bar{p}}^{-0.6} + x_{\bar{p}}^{-0.03})$ for the k_t-factorization approach, where $x_{\bar{p}}$ is a parton momentum fraction in the antiproton.

The formula above is a purely mathematical fit which applies in a limited range of $x_{\bar{p}}$. This formula should not be extrapolated toward very small values of $x_{\bar{p}}$. Beyond the experimental Tevatron region, our formula has no physical meaning. Our fit nicely describes the CDF data at $\sqrt{s} = 1.8$ TeV. In our present fit, the gap survival factor depends somewhat arbitrarily on the parton momentum fraction in the antiproton. We wish to check if such a dependence could modify the measured distributions in the rapidity and transverse momentum of jets. Models motivated by the theory of dynamics of such a process should be considered in this context in the future.

In Fig. 10, we again show the distribution in $\bar{E}_T$ for the collinear (left panel) and k_t-factorization (right panel) approaches. The inclusion of the dependence of S_G on $x_{\bar{p}}$ improves the overall agreement with the CDF data.

In Fig. 11, we show similar distributions in $\bar{\eta}$. One can observe a sizable shift of the distributions toward larger $\bar{\eta}$.

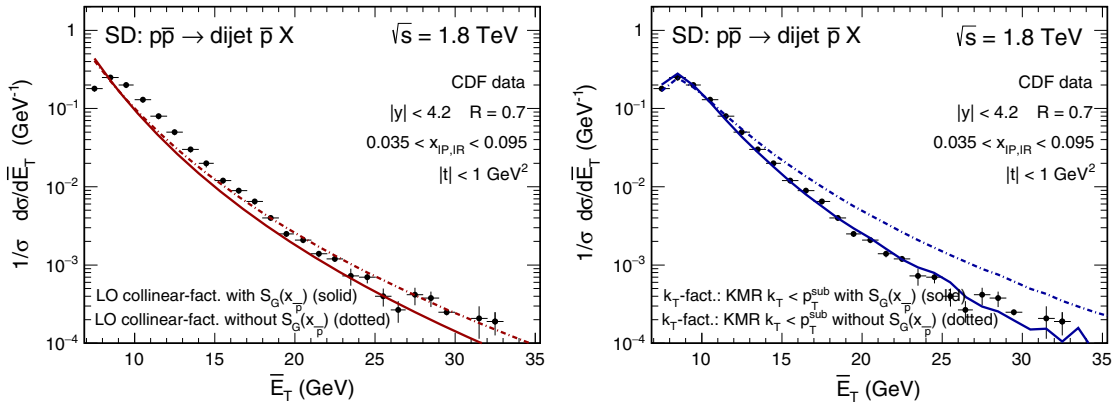

FIG. 10. $\bar{E}_T$ distribution for collinear (left panel) and k_t-factorization (right panel) approaches with and without the inclusion of the dependence of S_G on $x_{\bar{p}}$.

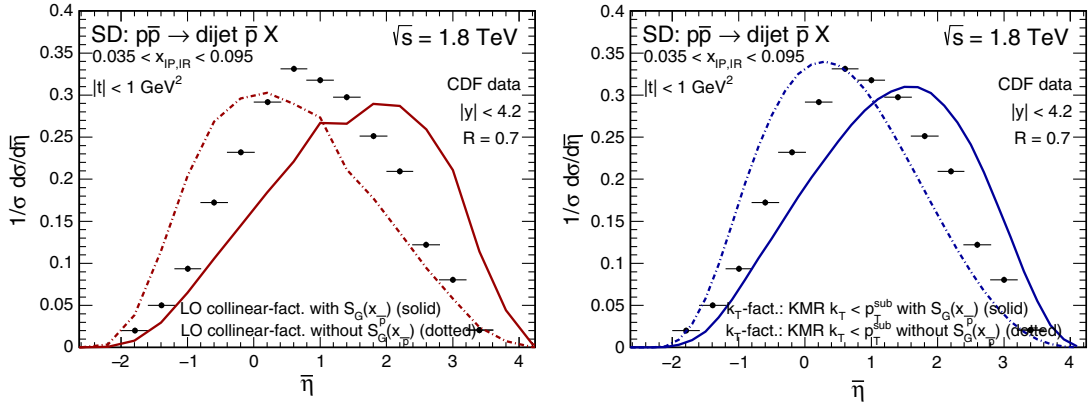

FIG. 11. $\bar{\eta}$ distribution for collinear (left panel) and k_t-factorization (right panel) approaches with and without the inclusion of the dependence of S_G on $x_{\bar{p}}$.

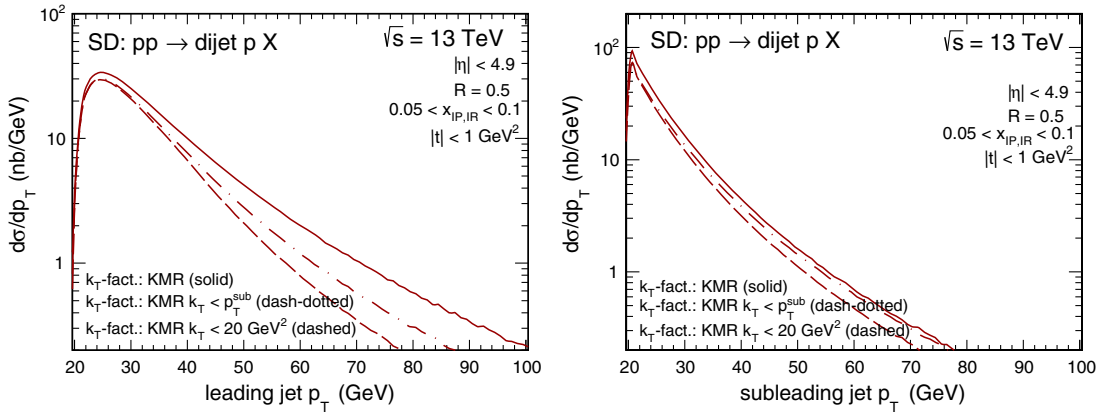

FIG. 12. Distribution in the jet transverse momentum for leading (left panel) and subleading (right panel) jets for $\sqrt{s} = 13$ TeV and for the ATLAS cuts. Here, $S_G = 0.05$.

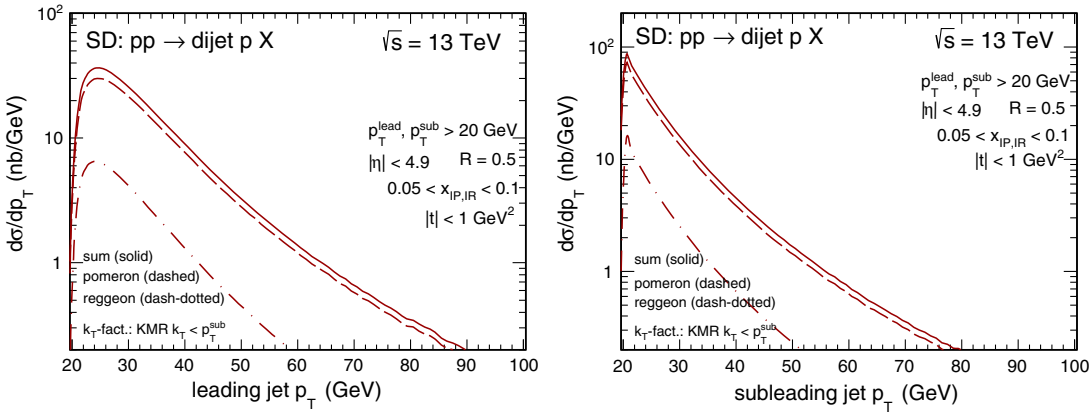

FIG. 13. The contribution of the Pomeron and subleading Reggeon for transverse momentum distribution for the leading (left panel) and subleading (right panel) jets for $\sqrt{s} = 13$ TeV and for the ATLAS cuts. Here, $S_G = 0.05$.

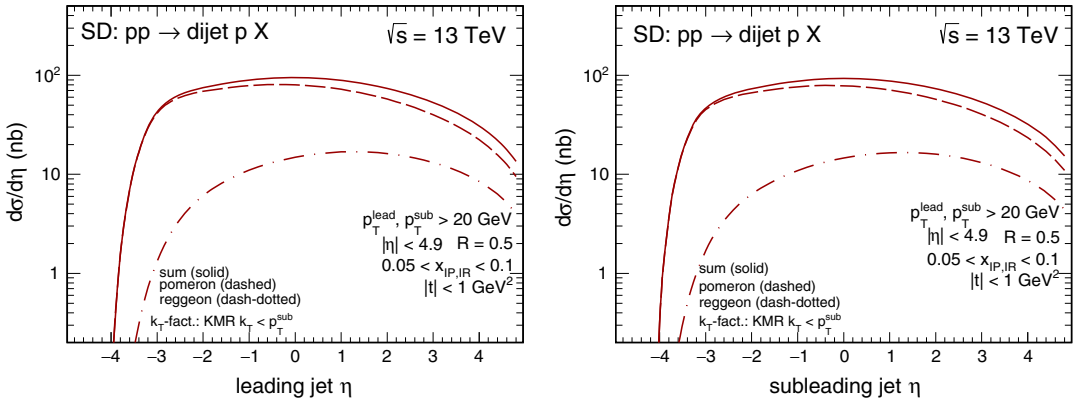

FIG. 14. Distribution in the jet rapidity for leading (left panel) and subleading (right jet) jets for $\sqrt{s} = 13$ TeV. Here, $S_G = 0.05$.

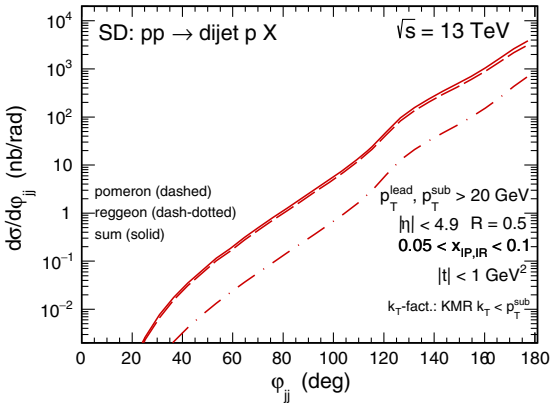

FIG. 15. Our predictions for azimuthal angle correlations between the leading and subleading jets. Here, $S_G = 0.05$.

The shift is in a correct direction but is much too big. This should be traced back to the extreme assumption of the dependence of S_G on $x_{\bar{p}}$ only. In reality, S_G may depend on a few kinematical variables. However, such a study goes far beyond the scope of the present paper.

According to our knowledge, there is no commonly accepted theory of the gap survival factor. Our trial in this section of the paper is purely phenomenological and demonstrates the potential importance of the dependence of S_G on kinematical variables for the description of real data.

C. Predictions for the LHC

In this subsection, we wish to present our results for the LHC energy $\sqrt{s} = 13$ TeV. In our calculations, we use cuts relevant for the planned ATLAS experiments, so we use a range of rapidities relevant for the ATLAS experiment $-4.9 < y_1, y_2 < 4.9$. We consider a rather low cut on the transverse momenta of jets $p_t > 20$ GeV. In the following, we shall use $S_G = 0.05$.

In Fig. 12, we show distribution in jet transverse momentum, for leading (left panel) and subjeading (right panel) jets. As for the Tevatron, we discuss the role of extra cuts on parton transverse momenta. The cuts have a bigger effect on leading jets.

In Fig. 13, we compare contributions of the Pomeron and subleading Reggeon for the ATLAS range of $x_{IP,IR}$. The subleading contribution is somewhat larger than 10%.

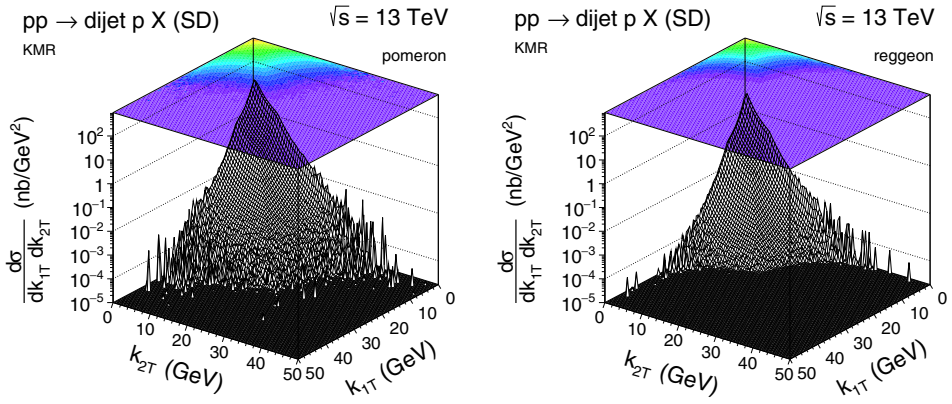

FIG. 16. Two-dimensional distributions in parton transverse momenta for the Pomeron (left panel) and subleading Reggeon (right panel). In this calculation, $\sqrt{s} = 13$ TeV and ATLAS cuts were imposed. Here, $S_G = 0.05$.

TABLE I. The calculated cross sections in microbarns for single-diffractive production of dijets in pp-scattering at $\sqrt{s} = 13$ TeV for different cuts on transverse momentum of the dijets. Here, the rapidity of the dijets is $|y^{jet}| < 4.9$, that corresponds to the ATLAS detector acceptance. The cross section here is not multiplied by the gap survival factors.

	Collinear		k_T-fractorization approach	
$p_{T,\min}^{\text{jet}}$ cuts	MMHT2014nlo	KMR	KMR $k_T < p_{T,\min}^{\text{jet}}$ (IP)	KMR $k_T < p_{T,\min}^{\text{jet}}$ (IR)
$p_T^{\text{jet}} > 20$ GeV	9.08	11.42	8.53	1.79
$p_T^{\text{jet}} > 35$ GeV	2.34	3.89	3.98	0.62
$p_T^{\text{jet}} > 50$ GeV	0.42	0.83	0.68	0.16

There is no evident dependence on the value of the transverse momentum.

In Fig. 14, we show similar distributions for jet rapidity again for the leading and subleading jets. As before, we show contributions of the Pomeron and subleading Reggeon separately. Here, the relative contribution of the subleading Reggeon is an evident function of rapidity, both for the leading and subleading jets.

Azimuthal angle correlations between the leading and subleading jets are shown in Fig. 15. Similar shapes are obtained for Pomeron and Reggeon contributions.

Finally, in Fig. 16, we show purely theoretical two-dimensional distributions in transverse momenta of partons for the Pomeron (left panel) and subleading Reggeon (right panel), respectively, for nondiffractive and diffractive sides. As for the Tevatron, the distributions are surprisingly symmetric in k_{1T} and k_{2T}. In this calculation, no extra cuts on parton transverse momenta have been imposed. We stress that very large transverse momenta of partons enter the considered dijet production.

In Table I, we present the integrated cross section for the ATLAS acceptance for single-diffractive production of dijets for different cuts of the jet-p_T.

IV. CONCLUSIONS

In the present paper, we have presented for the first time results for the single-diffractive production of dijets within the k_t-factorization approach. The resolved Pomeron model with flux of the Pomeron and Reggeon and parton distribution in the Pomeron have been used. The diffractive unintegrated parton distributions were obtained based on their collinear counterparts. The latter were used to fit the HERA data for the diffractive F_2 structure function and for diffractive dijet production. The rapidity gap is not calculated but can be fitted to the data. A constant value has been assumed as a default.

Results of our calculations were compared with the Tevatron data where forward antiprotons and rapidity gaps were measured. We have calculated distributions in $\bar{E}_T$ and $\bar{\eta}$. A reasonable agreement has been achieved. We have compared results obtained within collinear and k_t-factorization approaches. The k_t-factorization leads to a better description in E_T close to the lower transverse momentum cut.

Several other distributions have been presented and discussed, many of them for the first time.

It is rather difficult to describe the distributions in $x_{\bar{p}}$ with a constant value of the gap survival factor, especially for $\sqrt{s} = 1.8$ TeV. We have considered a possibility that the gap survival factor depends exclusively on $x_{\bar{p}}$ and studied consequences for other observables. A phenomenological $x_{\bar{p}}$ function was used to fit the Tevatron data. Such a dependence of the gap survival factor leads to an effective shift of the distribution in $\bar{\eta}$ in better agreement with the Tevatron data. Our preliminary study suggests that the dependence of gap survival factor on kinematical variables can be also an important ingredient in order to understand details of rapidity distributions. Clearly, further studies are necessary in the future.

We have also made predictions for future LHC measurements. Several differential distributions have been presented. We hope for their verification in the near future.

ACKNOWLEDGMENTS

This study was partially supported by the Polish National Science Centre Grants No. DEC-2013/09/D/ST2/03724 and No. DEC-2014/15/B/ST2/02528.

[1] M. Klasen and G. Kramer, Eur. Phys. J. C **38**, 93 (2004).
[2] A. B. Kaidalov, V. A. Khoze, A. D. Martin, and M. G. Ryskin, Eur. Phys. J. C **66**, 373 (2010).
[3] M. Klasen and G. Kramer, Eur. Phys. J. C **70**, 91 (2010).
[4] V. Guzey and M. Klasen, Eur. Phys. J. C **76**, 467 (2016).
[5] R. B. Appleby and J. R. Forshaw, Phys. Lett. B **541**, 108 (2002).
[6] A. B. Kaidalov, V. A. Khoze, A. D. Martin, and M. G. Ryskin, Phys. Lett. B **559**, 235 (2003).
[7] M. Klasen and G. Kramer, Phys. Rev. D **80**, 074006 (2009).
[8] C. Royon, arXiv:1310.4675.
[9] C. Marquet, C. Royon, M. Saimpert, and D. Werder, Phys. Rev. D **88**, 074029 (2013).
[10] F. Abe *et al.* (CDF Collaboration), Phys. Rev. Lett. **79**, 2636 (1997).
[11] T. Affolder *et al.* (CDF Collaboration), Phys. Rev. Lett. **84**, 232 (2000).
[12] T. Affolder *et al.* (CDF Collaboration), Phys. Rev. Lett. **85**, 4215 (2000).
[13] T. Affolder *et al.* (CDF Collaboration), Phys. Rev. Lett. **84**, 5043 (2000).
[14] D. Acosta *et al.* (CDF Collaboration), Phys. Rev. Lett. **88**, 151802 (2002).
[15] M. H. L. S. Wang *et al.*, Phys. Rev. Lett. **87**, 082002 (2001).
[16] T. Affolder *et al.* (CDF Collaboration), Phys. Rev. Lett. **87**, 241802 (2001).
[17] T. Aaltonen *et al.* (CDF Collaboration), Phys. Rev. Lett. **99**, 242002 (2007).
[18] T. Aaltonen *et al.* (CDF Collaboration), Phys. Rev. D **77**, 052004 (2008).
[19] T. Aaltonen *et al.* (CDF Collaboration), Phys. Rev. D **82**, 112004 (2010).
[20] T. Aaltonen *et al.* (CDF Collaboration), Phys. Rev. Lett. **108**, 081801 (2012).
[21] I. Babiarz, R. Staszewski, and A. Szczurek, Phys. Lett. B **771**, 532 (2017).
[22] S. Catani, M. Ciafaloni, and F. Hautmann, Phys. Lett. B **242**, 97 (1990).
[23] S. Catani, M. Ciafaloni, and F. Hautmann, Nucl. Phys. **B366**, 135 (1991).
[24] M. Luszczak, R. Maciula, A. Szczurek, and M. Trzebinski, J. High Energy Phys. 02 (2017) 089.
[25] M. A. Nefedov, V. A. Saleev, and A. V. Shipilova, Phys. Rev. D **87**, 094030 (2013).
[26] A. van Hameren, P. Kotko, and K. Kutak, Phys. Rev. D **88**, 094001 (2013); **90**, 039901(E) (2014).
[27] K. Kutak, R. Maciula, M. Serino, A. Szczurek, and A. van Hameren, J. High Energy Phys. 04 (2016) 175.
[28] K. Kutak, R. Maciula, M. Serino, A. Szczurek, and A. van Hameren, Phys. Rev. D **94**, 014019 (2016).
[29] G. Ingelman and P. E. Schlein, Phys. Lett. B **152**, 256 (1985).
[30] R. Maciula and A. Szczurek, Phys. Rev. D **87**, 094022 (2013).
[31] M. A. Kimber, A. D. Martin, and M. G. Ryskin, Phys. Rev. D **63**, 114027 (2001).
[32] G. Watt, A. D. Martin, and M. G. Ryskin, Phys. Rev. D **70**, 014012 (2004); Phys. Rev. D **70**, 079902(E) (2004).
[33] S. Catani, M. Ciafaloni, and F. Hautmann, Phys. Lett. B **307**, 147 (1993).
[34] A. Aktas *et al.* (H1 Collaboration), Eur. Phys. J. C **48**, 715 (2006).
[35] L. A. Harland-Lang, A. D. Martin, P. Motylinski, and R. S. Thorne, Eur. Phys. J. C **75**, 204 (2015).
[36] R. Maciula and A. Szczurek, Phys. Rev. D **94**, 114037 (2016).